# CHAPTER – 6

## Synthesis and Characterization of Li- substituted Magnetite Nanoparticles

## 6.1 Introduction

The substitutions of tetravalent, trivalent and bivalent ions in magnetite nanoparticles have displayed the $T_S$ values near 42 - 46 °C during MHT (chapters 3, 4 and 5). However, it has been described in the last three chapters that the $T_S$ value was attained for a particular combination of frequency and amplitude of the fields and this combination is different for different dopant ions or their concentration. The present chapter deals with the effect of monovalent ion ($Li^+$) substitution on heating ability of the magnetite nanoparticles. The nanoparticles of $Li_xFe_{3-x}O_4$ (0.06, 0.1, and 0.3) were also prepared by microwave refluxing method.

# 6.2 Li substituted magnetite nanoparticles

## 6.2.1 XRD Study

The X-ray diffraction patterns (Fig.6.2.1) for $Li_xFe_{3-x}O_4$ ($x$ = 0.06, 0.1 and 0.3) samples displayed the single phase nature which suggest the substitution of Fe-ions by Li-ions.

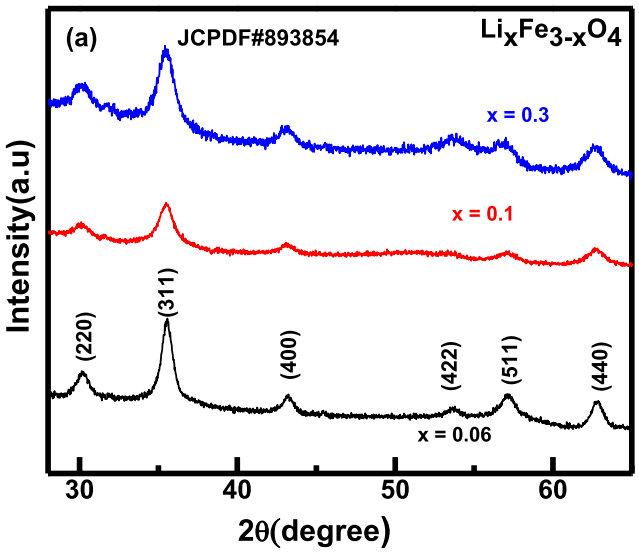


Fig. 6.2.1: X-ray diffraction patterns for $Li_xFe_{3-x}O_4$ ($x$ = 0.06, 0.1 and 0.3) samples.

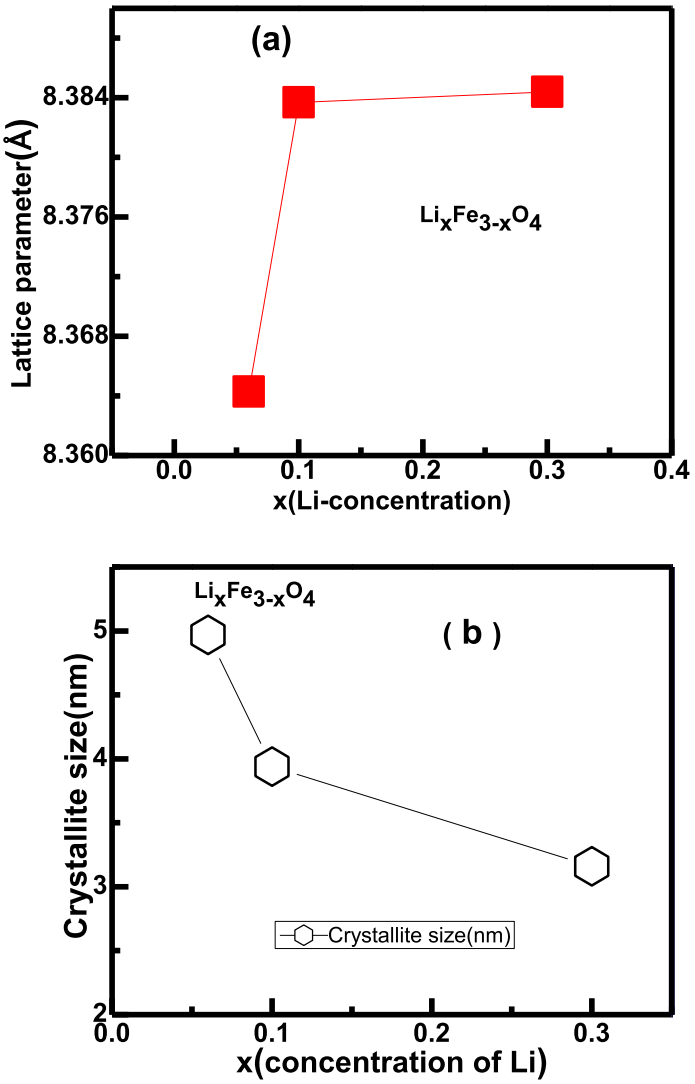


Fig 6.2.2: variation with increased Li content in (a) lattice parameter, (b) crystallite size.

The continuous increase of the lattice parameter from 8.363 to 8.381 Å for $x = 0.06$ and $x = 0.3$ samples were observed. This may be due to larger ionic radius of Li-ions which substituted $Fe^{3+}$ ions from octahedral positions of spinel structure. The average crystallite size of the samples was ~ 4 nm. It has been observed that $LiFeO_2$ phase was also present along with magnetite phase for $x = 0.5$ (figure not shown). Due to this, poor $M_S$ value for this sample was obvious and hence other characterizations for this sample were not done.

### 6.2.2. TEM study

The TEM bright field images of (Figs. 6.2.2 a & b) displayed the spherical morphology of $Li_{0.06}Fe_{2.94}O_4$ and $Li_{0.3}Fe_{2.72}O_4$ nanoparticles which were produced by microwave refluxing method (chapter 2). The SAD patterns (inset images of Figs. 6.2.2 a & b) indicated the FCC structure of the samples. The particles size of $x$ = 0.06 and 0.3 samples was found to be in the range of 6-22 nm and 4-11 nm respectively.

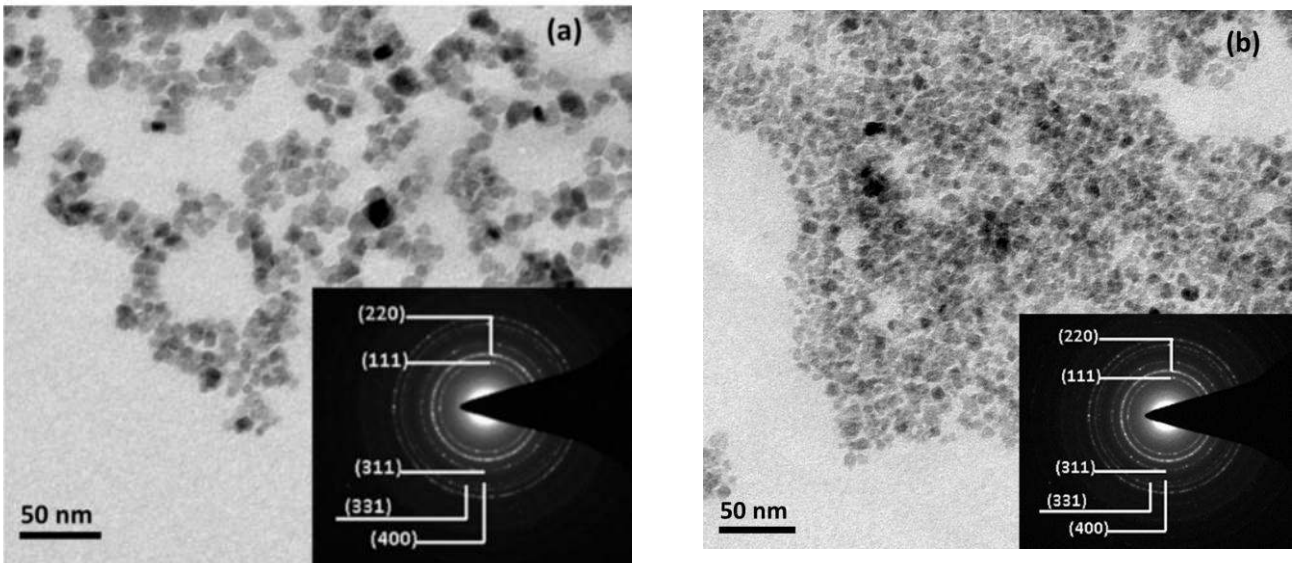


Fig. 6.2.3: TEM brightfield image of (a) $Li_{0.06}Fe_{2.94}O_4$ and (b) $Li_{0.3}Fe_{2.7}O_4$ samples (Inset shows corresponding SAD pattern).

### 6.2.3. XPS study

Fig. 6.2.3 presents the XPS spectra of $Li_{0.3}Fe_{2.7}O_4$ sample. The Fe 2p spectra indicated that the presence of both $Fe^{2+}$ and $Fe^{3+}$ ions in the sample. The core level Li 1s spectra displayed the presence of peaks at 58 and 55 eV which correspond to the $Li_2CO_3$ and $Li_2O$[79]. This indicates the presence Li in +1 state. The deconvoluted O 1s spectrum

present the peaks at 529.5, 531.3, 533 and 534 eV which may be attributed to lattice oxygen, adsorbed oxygen and water molecules respectively[80].

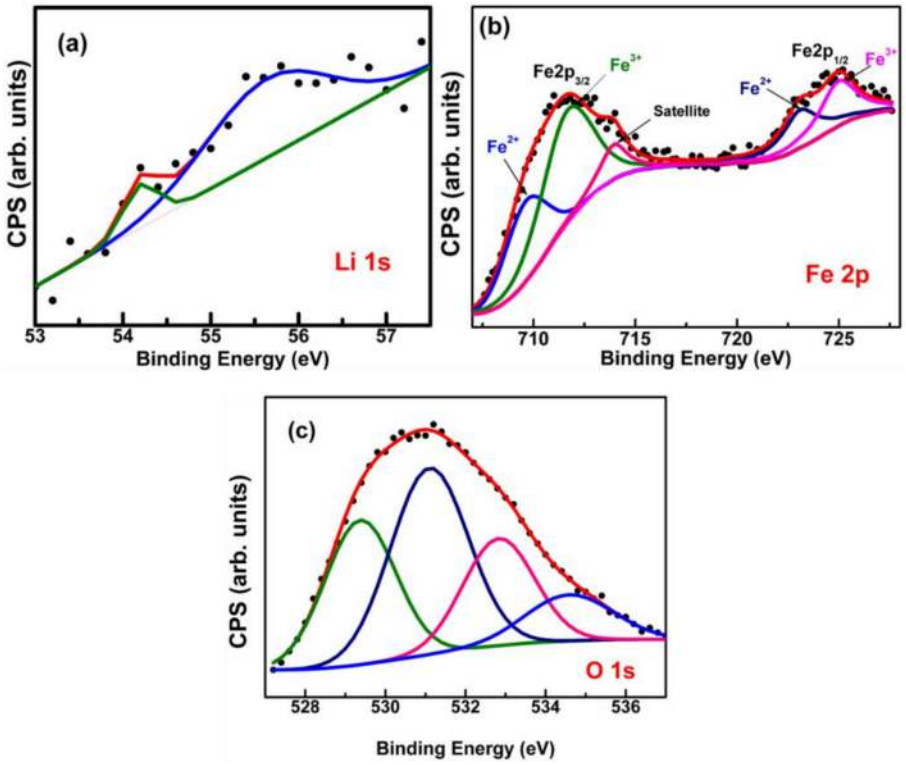


Fig. 6.2.4: XPS spectra of $Li_{0.3}Fe_{2.7}O_4$ sample (a) Fe 2p (b) Li 1s and(c) O1s core level spectra.

## 6.2.4. Magnetization study

Figure 6.2.4 presents the room temperature M vs. H curves for $Li_xFe_{3-x}O_4$ ($x$ = 0.06, 0.1 and 0.3) samples. There was a continuous decrease in $M_S$ value with increased Li concentration. The $M_S$ values were 54.1, 48.6, 40.9 $Am^2/kg$ for $x$ = 0.06, 0.1 and 0.3 respectively. Such a decrease could be due to the occupancy of $Li^+$ ions at the octahedral sites which effectively reduces the overall magnetization of the sample.

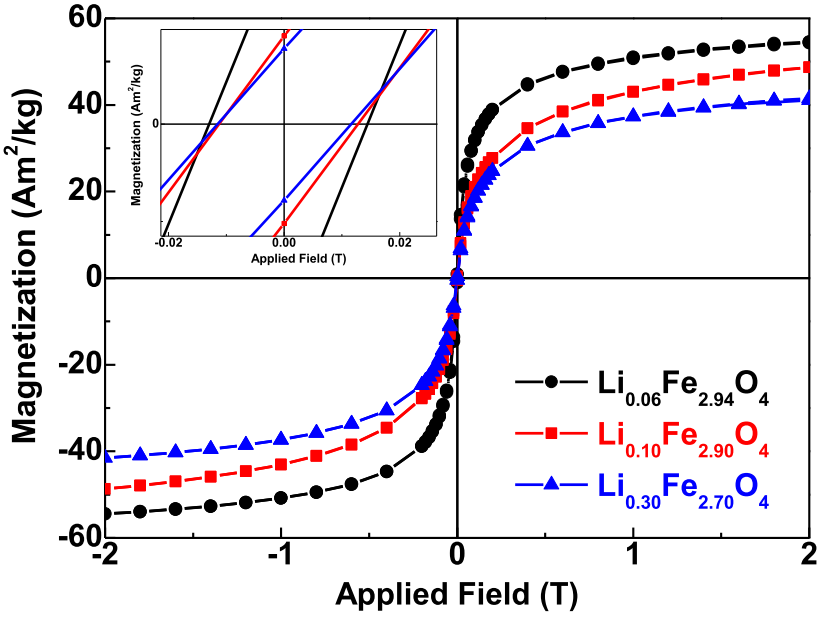


Fig.6.2.5: Room temperature magnetization vs. field curves for $Li_xFe_{3-x}O_4$ ( $x$ = 0.06, 0.1 and 0.3) samples.

The $H_C$ values were 13, 12 and 11 Oe for $x$ = 0.06, 0.1 and 0.3 samples respectively. Similarly, the $M_r$ values for the samples $x$ = 0.06, 0.1 and 0.3 were 0.9, 0.45, 0.39 $Am^2/kg$ respectively. These values suggest that the samples essentially had ferrimagnetic component despite their size below 20 nm.

## 6.2.5. Mössbauer spectroscopy study

The Mössbauer spectra recorded at room temperature for composition $x$ = 0.06, 0.1, and 0.3 are presented in Fig. 6.2.5. The values of hyperfine field (BHF), isomer shift ($\delta$), quadrupole splitting ($\Delta$), line width ($\Gamma$) and relative areas ($R_A$) for the samples are given in table 6.1. The Mössbauer spectra of $Li_{0.06}Fe_{2.94}O_4$ sample could be fitted with three sextets (six lines Zeeman splitting patterns) and one doublet. Out of the two sextets one was assigned to $Fe^{3+}$-ions in the tetrahedral site whereas another one was for both $Fe^{3+}$ -ions and $Fe^{2+}$ -ions at the octahedral site. Moreover, the decrease in hyperfine field steeply at the latter site suggests that the $Li^+$-ions mostly prefer the octahedral sites (Figs. 6.2.5 and

6.2.6 a). The third sextets were observed for superparamgantic component which was also observed for other samples discussed in earlier chapters. The samples with $x$ = 0.1 and 0.3 were also fitted with three sextets and a doublet (Fig. 6.2.5). The doublets were observed due to the presence of superparamagnetic relaxation phenomenon. The continuous decrease in hyperfine fields values for sample $x$ = 0.1 and 0.3 were observed for the sextet representing the octahedral site (Fig. 6.2.6 a).

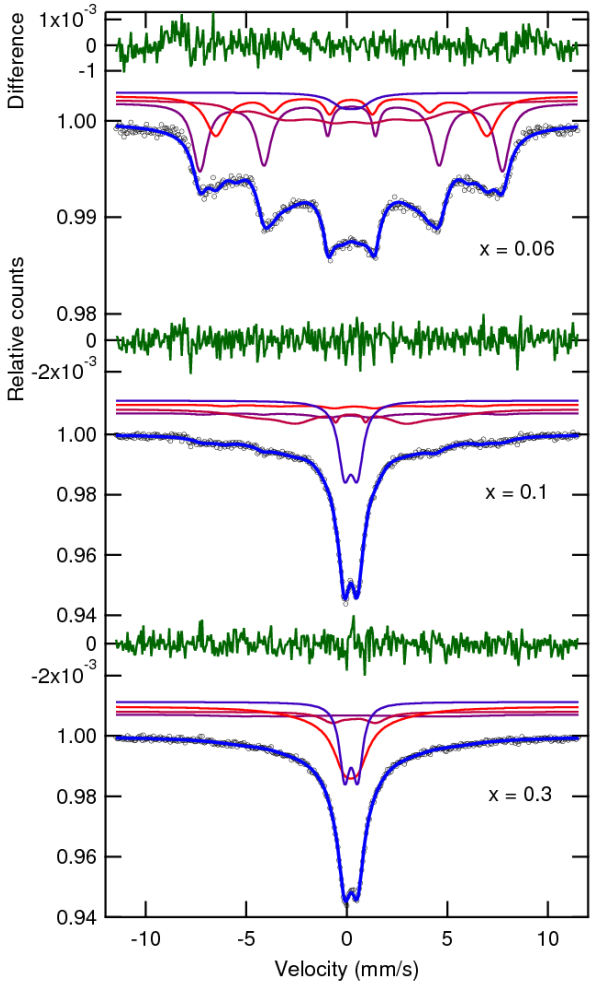


Fig. 6.2.5: Mössbauer spectra of $Li_xFe_{3-x}O_4$ samples (x = 0.06, 0.1 and 0.3).

The isomer shift was corroborated due to the presence of asymmetry arose from tetrahedral and octahedral sites Fe-ions[69]. The decrease in the IS values for octahedral

site was confirmed the presence of Li-ions. As discussed before, at higher concentration Li-ions occupied both the sites. Therefore, IS values were found to be increasing at octahedral site but decreasing at tetrahedral site with increased Li-ions concentration (6.2.6 b). The variations of Quadrupole splitting values with Li substitution are shown in Fig. 6.2.6 c. The obvious higher values were observed for doublets because MNPs were superparamagnetic components.

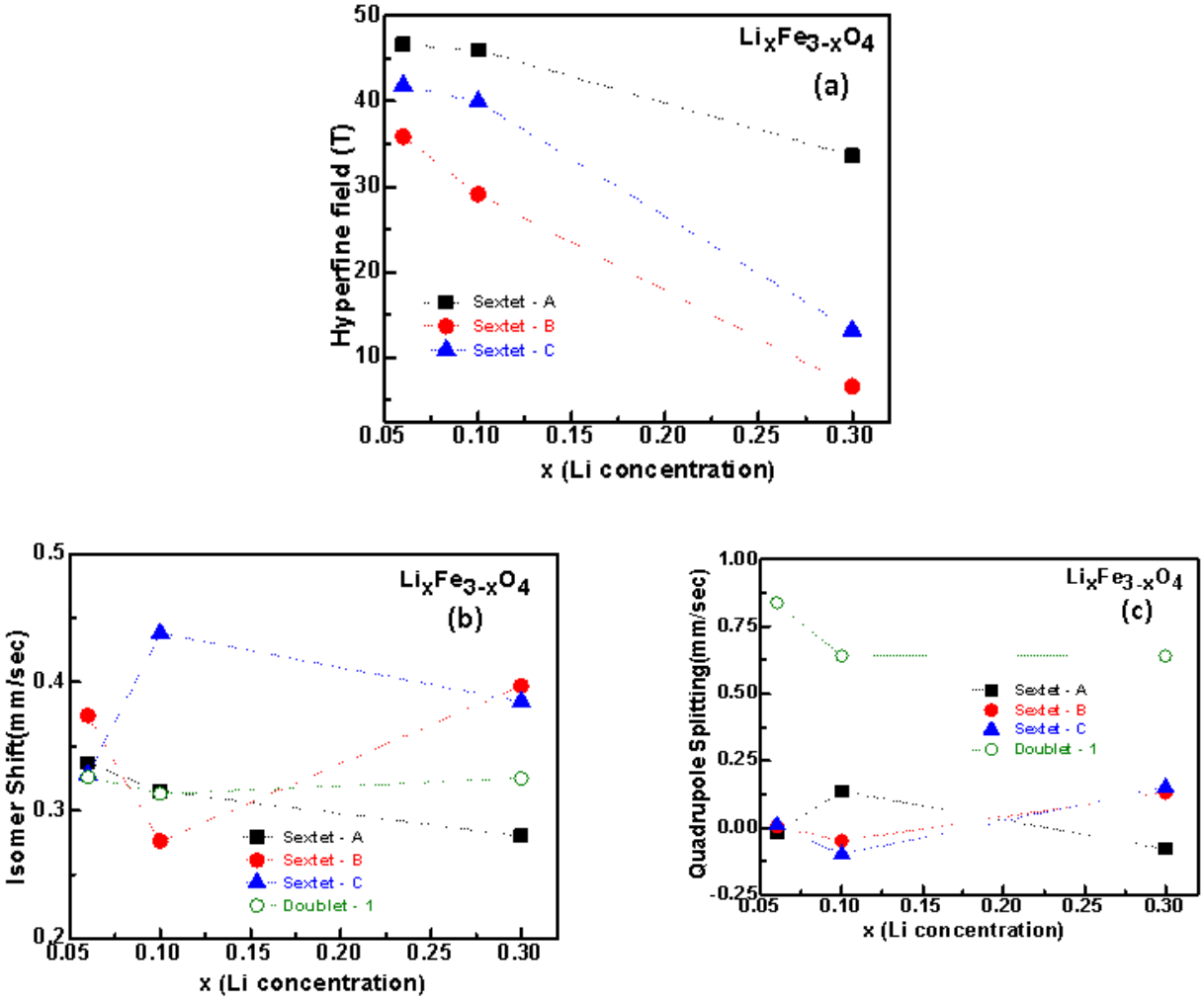


Fig. 6.2.6: Variation in (a) hyperfine field (b) isomer shift and (c) Quadrupole splitting and for $Li_xFe_{3-x}O_4$ ($x$ = 0.06, 0.1 and 0.3) samples.

Table 6.1:The values of hyperfine field (BHF), isomer shift ($\delta$), quadrupole splitting ($\Delta$), linewidth ($\Gamma$) and relative areas ($R_A$) in percentage of tetrahedral A ($Fe^{3+}$, $Fe^{3+}$) and octahedral B sites of ($Fe^{3+}$, $Fe^{2+}$) ions for $Li_xFe_{3-x}O_4$ ($x$ = 0.06, 0.1 and 0.3) samples derived from Mössbauer spectra recorded at room temperature

| **Sample Comp. (x)** | **Iron Sites** | **Hyper. field, ($H_{hf}$) Tesla(±0.2)** | **Quadrupole splitting, (Δ) mm/s(±0.01)** | **Isomer shift (δ) mm/s(±0.01)** | **Line width(Γ ) mm/s(±0.1)** | **Area ($R_A$) %** | **Fitting quality ($\chi^2$)** |
|---|---|---|---|---|---|---|---|
| 0.06 | Sextet A ($Fe^{3+}$) | 46.64 | -0.02 | 0.33 | 0.424 | 16.2 | 1.1762 |
| | Sextet B ($Fe^{3+,}$ $Fe^{2+}$) | 35.85 | 0.004 | 0.37 | 2.39 | 66.6 | |
| | Sextet C ($Fe^{3+}$) | 41.8 | 0.016 | 0.32 | 0.625 | 13.4 | |
| | Doublet ($Fe^{3+}$) | -- | 0.839 | 0.22 | 1.57 | 3.33 | |
| 0.1 | Sextet A ($Fe^{3+}$) | 45.98 | 0.135 | 0.31 | 1.57 | 25.2 | 0.9599 |
| | Sextet B ($Fe^{3}$) | 29.11 | -0.05 | 0.27 | 0.313 | 26.9 | |
| | Sextet C ($Fe^{3+,}$ $Fe^{2+}$) | 39.6 | -0.102 | 0.43 | 1.161 | 16.4 | |
| | Doublet ($Fe^{3+}$) | -- | 0.64 | 0.31 | 0.73 | 31.3 | |
| 0.3 | Sextet A ($Fe^{3+}$) | 33.58 | -0.08 | 0.28 | 1.86 | 8.85 | 1.1259 |
| | Sextet B ($Fe^{3+}$,$Fe^{2+}$) | 6.64 | 0.13 | 0.39 | 0.42 | 14.3 | |
| | Sextet C ($Fe^{3+}$) | 13.19 | 0.15 | 0.27 | 0.32 | 69.18 | |
| | Doublet ($Fe^{3+}$) | -- | 0.64 | 0.32 | 0.60 | 7.67 | |

## 6.2.6 Induction heating analysis

Figure 6.2.7a displayed the temperature vs. time curves for $Li_xFe_{3-x}O_4$ ( $x$ = 0.06, 0.1 and 0.3) samples at a field of amplitude 17 mT and a frequency of 338 kHz. For lower concentration of Li substituted sample ($x$ = 0.06) exhibited continuous rise in the temperature. In contrast, the $x$ = 0.1 and 0.3 samples show $T_S$ values at 50 and 26 °C respectively. Such a small $T_S$ value (~26 °C) was not observed for tetravalent, trivalent or divalent substituted $Fe_3O_4$ samples. The reported lowest $T_S$ value is ~ 32 °C which was observed for the Ce substituted $Fe_3O_4$ samples [66]. For tetravalent substituted $Fe_3O_4$, $Zr_{0.01}Fe_{2.99}O_4$ sample exhibited lowest $T_S$ value of ~ 29 °C at a field of amplitude 23 mT and a frequency of 173 kHz (chapter-3). In addition, divalent substituted $Fe_3O_4$, $Zn_xFe_{3-x}O_4$ for $x$ = 0.07 and 0.8 samples exhibited $T_S$ values of 28 and 29 °C respectively at a field of amplitude 17 mT and a frequency of 170 kHz (chapter-5). However, the $T_S$ values below 42 °C are not suitable for the practical applications. Figure 6.2.7b indicates that the $T_S$ values for the samples were in the range between 18 and 60 °C. Some of the $T_S$ values were much smaller than that of other samples (chapters 3, 4 and 5). However, all $T_S$ values do not lie in the range of therapeutic temperature (42 to 46 °C) like tetravalent, trivalent and divalent substituted magnetite samples. But, it is well known that these $T_S$ values can be enhanced by increasing power of magnetic field and then the Li substituted magnetite samples may also be useful for MHT applications.

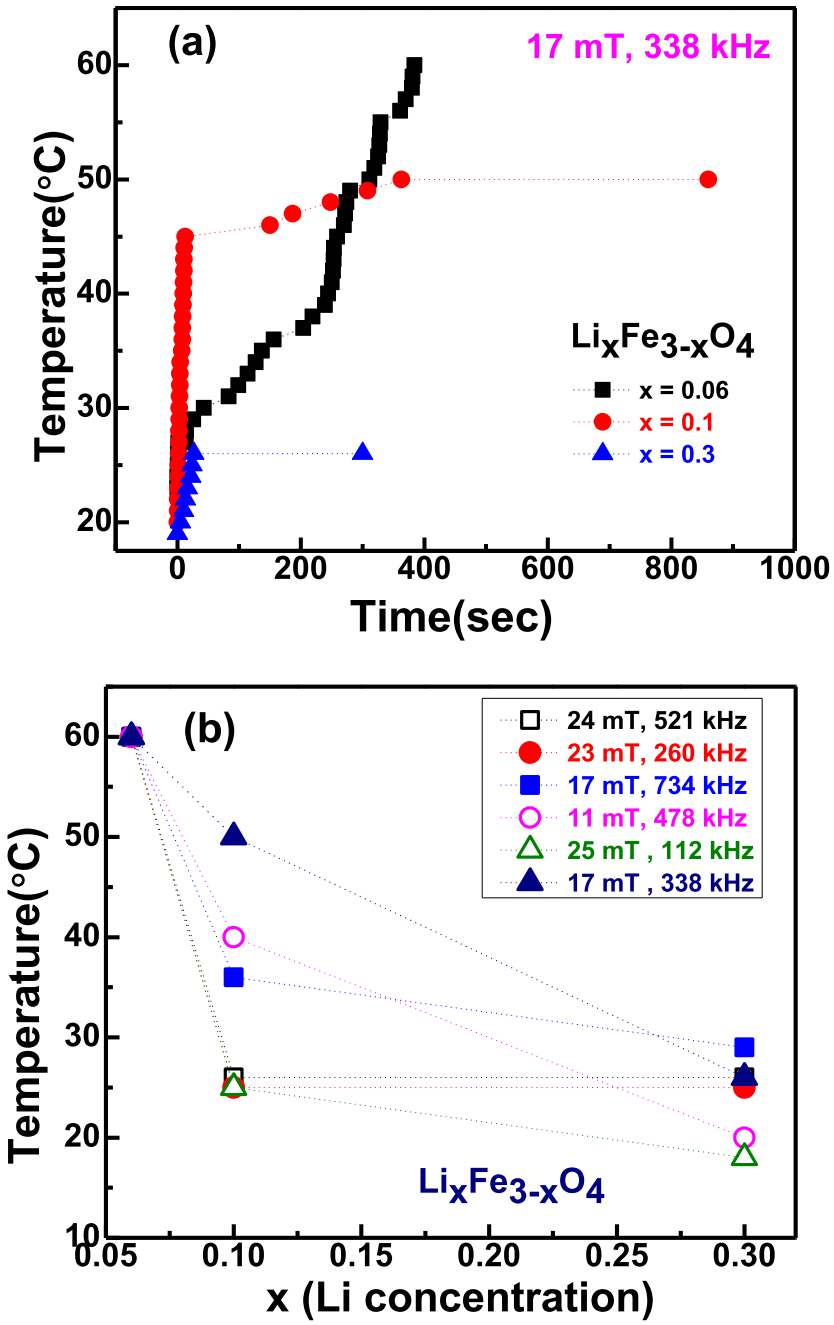


Fig. 6.2.7: (a) T vs. t curves at a field of amplitude of 24 mT and a frequency of 521 kHz and (b) $T_S$ values obtained during magnetic hyperthermia at different fields and frequencies for $Li_xFe_{3-x}O_4$ ($x$ = 0.06, 0.1 and 0.3) samples.

Fig. 6.2.8 presents the SAR values for $Li_xFe_{3-x}O_4$ ($x$ = 0.06, 0.1 and 0.3) ferrofluids at various magnetic fields. Considerably highest SAR value was observed for $x$ = 0.1 sample at 17 mT. However, the $M_S$ value for this sample was relatively lower than that of $x$ = 0.06 sample. This suggests that the SAR values not only depend upon the $M_S$ value but also on other factors such as type, quantity, morphology and polydispersity of the MNPs. It is clear from Fig. 6.2.8 that the SAR values also depend on amplitude and frequency of the applied AC magnetic fields. It is worthwhile to mention that the SAR values for $x$ = 0.1 samples was significantly higher than that of other samples (tetravalent, trivalent and divalent substituted magnetite).

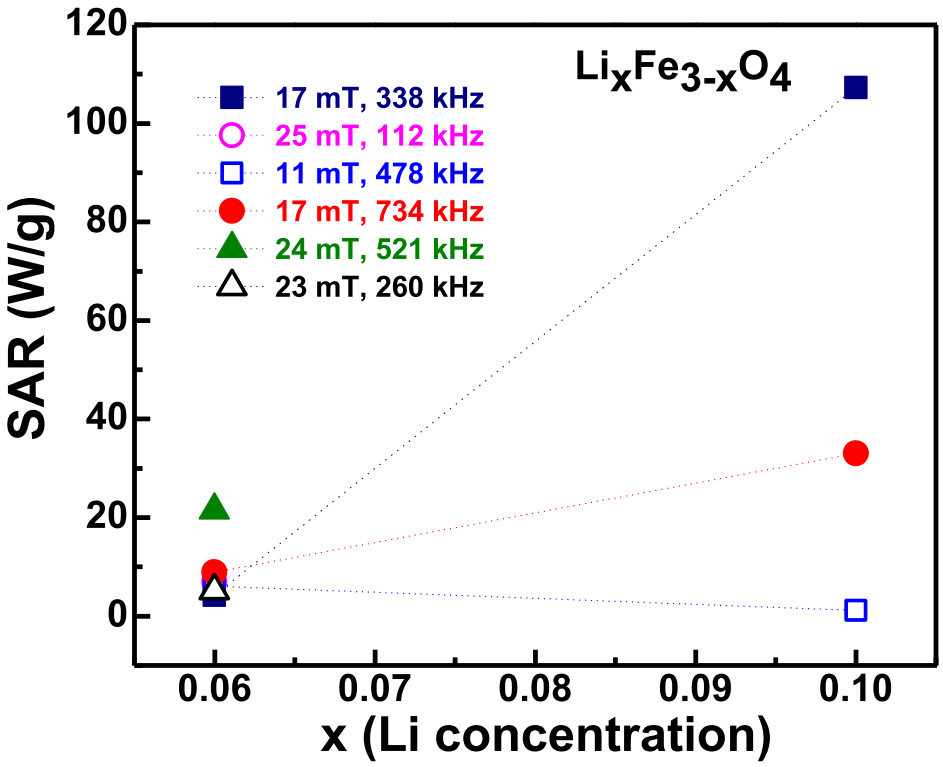


Fig. 6.2.8: The SAR values vs. Li concentration of $Li_xFe_{3-x}O_4$ ($x$ = 0.06, 0.1 and 0.3) samples at different field and frequencies.

It has been stated in earlier chapters that only the substituted $Fe_3O_4$ samples displayed the $T_S$ values during MHT but not the unsubstituted one. However, the exact reasons for obtaining such $T_S$ values are not well understood.

## 6.4 Conclusions

Nanoparticles of $Li_xFe_{3-x}O_4$ ($x$ = 0.06, 0.1 and 0.3) samples were synthesized via microwave refluxing technique. These particles had spherical morphology and the size was in the range of 6 to 13 nm. The monovalent ion substitution has continuously decreases the $M_S$ value of magnetite. This could be due to the occupancy of the Li-ions in octahedral sites of $Fe_3O_4$. All the samples exhibited stabilization temperature at various field and frequencies of AC magnetic fields. The SAR values of the samples relatively larger than that of tetravalent, trivalent and divalent substituted magnetite samples.